

Cation spin and superexchange interaction in oxide materials below and above spin crossover under high pressure.

Vladimir A. Gavrichkov,* Semyon I. Polukeev, and Sergey G. Ovchinnikov
Kirensky Institute of Physics, Akademgorodok 50, bld.38, Krasnoyarsk, 660036 Russia
 (Dated: February 13, 2020)

We derived simple rules for the sign of 180° superexchange interaction based on the multielectron calculations of the superexchange interaction in the transition metal oxides that are valid both below and above spin crossover under high pressure. The superexchange interaction between two cations in d^n configurations is given by a sum of partial contributions related to the electron-hole virtual excitations to the different states of the d^{n+1} and d^{n-1} configurations. Using these rules, we have analyzed the sign of the 180° superexchange interaction of a number of oxides with magnetic cations in electron configurations from d^2 till d^8 : the iron, cobalt, chromium, nickel, copper and manganese oxides with increasing pressure. The most interesting result concerns the magnetic state of cobalt and nickel oxides CoO , Ni_2O_3 and also La_2CoO_4 , LaNiO_3 isostructural to well-known high- T_C and colossal magnetoresistance materials. These oxides have a spin $\frac{1}{2}$ at the high pressure. Change of the interaction from antiferromagnetic below spin crossover to ferromagnetic above spin crossover is predicted for oxide materials with cations in d^5 (FeBO_3) and d^7 (CoO) configurations, while for materials with the other d^n configurations spin crossover under high pressure does not change the sign of the 180° superexchange interaction.

I. INTRODUCTION

The mechanism of superexchange interaction is well known for a long time¹. The effective Heisenberg Hamiltonian describes the exchange interaction J of the magnetic cations in the ground state. It is well known that there are many excited states for multielectron cations.² However these states are not involved by the superexchange interaction, and Heisenberg model is based theory because typically excited states lies well above the magnetic scale J and Curie/Neel temperatures (T_C/T_N). A low energy description of magnetic insulators may be violated in two situations. The first one is related with intensive optical pumping when one of magnetic cations is excited into some high energy state and its exchange interaction with the neighbor cation in the ground state changes³ resulting in many interesting effects of the femtosecond magnetism.^{4,5} The other situation occurs at the high pressure when the cation spin crossover in magnetic insulators from the high spin (HS) to the low spin (LS) state takes place.^{2,6} The spin crossover occurs due to competition between the energy of the crystalline field $10Dq$ and the parameter of intratomic Hund exchange J_H . Typically, the applied pressure increases the crystal field, but does not significantly change the exchange parameter J_H . The spin crossovers are known for many transition metal oxides with $d^4 \div d^7$ cations, and for transition metal complexes, like metalorganic molecules or molecular assemblies.⁷⁻¹⁸ Near crossover the energies of two states ε_{HS} and ε_{LS} are close to each other and conventional scheme of the superexchange interaction calculation should be modified.

The spin crossovers have been experimentally detected and investigated in a number of transition metal oxides.⁷ Calculations also confirm a possibility of the spin crossovers in these materials and their role in the metal-insulator transition.^{5,19} In real, a situation is complicated

by the observed structural and chemical instabilities of some oxide materials at the high pressures,^{7,20} which destroy the possibility of a comparison between the calculation of superexchange interaction and experimental data. The results of the experimental studies contain both the examples of stable FeBO_3 with isostructural spin crossover⁶ at $\sim 60\text{GPa}$, and chemically unstable Fe_2O_3 hematite.²⁰ Further we will restrict ourselves to the stable oxide materials and assume that there are isostructural areas on the phase P/T diagram of the oxides, where the magnetic ordering is governed mainly by strong superexchange AFM interactions in Me-O-Me with a bond angle of about 180° .

The aim of our work is to answer the question of how the 180° superexchange interaction depends on the cation spin in transition metal oxides at the high pressure, and can simple changes in the crystal field without a spin crossover lead to a change in its nature from AFM to FM? In terms of the realistic p-d model that include d-electrons of cation and p-electrons of oxygen the superexchange interaction arises via cation-anion p-d hopping t_{pd} in the fourth order perturbation theory over the t_{pd} (see for example²¹⁻²⁴). Eliminating the oxygen states one can obtain the effective Hubbard model with cation-cation hopping $t \sim t_{pd}^2 / (\varepsilon_p - \varepsilon_d)$ and then the effective Heisenberg model may be obtained by the unitary transformation of the Hubbard model^{25,26} with the superexchange interaction of the kinematic origin $J \sim t^2/U$. The superexchange interaction appears in a second order perturbation theory over interband hopping t from the occupied low Hubbard band into the empty upper Hubbard band and back. It may be considered as result of the virtual excitation of the electron-hole pair.

We start discussing the properties of the transition metal oxides with a model of the periodic lattice of cations in d^n configuration in a center of oxygen octahedra with a set of states $|n\rangle$ with energy ε_n . The elec-

tron addition (extra electron) results in the d^{n+1} states $|e\rangle$ with energies $\varepsilon_e(n+1)$. Similar electron removal (or hole creation) involves the d^{n-1} states $|h\rangle$ with energies $\varepsilon_h(n-1)$. Thus, a partial contribution to the superexchange interaction involves 4 states: at site 1 creation of the electron excite the initial state $|n\rangle$ (we call this states neutral) into some $|e\rangle$ state (we call these excitation by electronic) and at site 2 the hole creation excites the neutral state into the one of the states $|h\rangle$ (we call them hole). These electron-hole excitations are virtual, after their annihilation back the final state is again two cations in initial d^n configurations. This approach allows us to consider all partial contributions to the superexchange interaction including both the ground states as well as excited states in all three sectors of the Hilbert space: neutral $N_0(d^n)$, electronic $N_+(d^{n+1})$ and hole $N_-(d^{n-1})$. Here we show that the sign of the partial contributions J_{ij}^{FM} and J_{ij}^{AFM} to the total superexchange interaction $J_{ij} = J_{ij}^{AFM} + J_{ij}^{FM}$ is directly independent on the cation spin $S(d^n)$, but is controlled by the spin ratio $S(d^{n-1}) = S(d^{n+1})$ (AFM interaction) or $S(d^{n-1}) = S(d^{n+1}) \pm 1$ (FM interaction). The crystal field perturbations, without a reversal of the electron spin, does not change the nature (sign) of partial contributions J_{ij}^{FM} and J_{ij}^{AFM} , however they can lead to a change in their relative magnitudes, as a result, to a change in the sign of superexchange parameter J_{ij} . A main factor for the comparison between the AFM and FM interactions is the type σ or π overlapping orbitals involved by the partial contributions. These characteristics is comparable in simplicity with the well known Goodenough-Kanamori-Anderson rules, which are used many years by scientists in the analysis of the magnetic states of dielectric materials.^{27,28} In the paper we also generalize the previous results for the superexchange interaction in iron borate under high pressure and optical pumping^{5,19} to the different transition metals oxides with magnetic ions in the $d^2 - d^8$ configurations.

For the readers convenience the theoretical details are placed in the Appendix below and in the main text will discuss the physical ideas.

II. ADDITIVITY PROPERTIES OF SUPEREXCHANGE INTERACTION

$$\delta\hat{H}_1 = \sum_{ij} \hat{h}_{ij}^{out} = \sum_{ij} \sum_{nhe} \left[t_{ij}^{el, hn} \sum_{\sigma} \alpha_{i\sigma}^+(en) \beta_{j\sigma}(hn) + t_{ij}^{nh, le} \sum_{\sigma} \beta_{i\sigma}^+(nh) \alpha_{j\sigma}(ne) \right], \quad (2)$$

that describes the creation and annihilation of the virtual electron (denoted by the operator $\alpha_{i\sigma}^+$) and hole (operator $\beta_{i\sigma}^+$) pairs. Exactly the virtual excitations through the dielectric gap Δ_{nhe} to the conduction band and vice versa in Eq.(2) contribute to the superexchange

We will work within a framework of the cell perturbation approach⁵ to calculate a magnitude of the superexchange, that logically fits into the LDA + GTB method to study both the electronic structure,^{29,30} and the 180° superexchange interaction in oxide materials under the pressure and optical pumping. The conclusion of our study will be some simple rules which can help to estimate the sign of the superexchange in the oxide materials at high pressure without complicate calculations. At this point we will take the superexchange Hamiltonian (1) (see Appendix) as a working tool, in structure which there is a summation over the independent contributions involving the ground $|n_0\rangle = |(N_0, M_S)_{n_0}\rangle$, excited electronic $|e(h)\rangle = |(N_{\pm}, M_S)_{e(h)}\rangle$ (e) and hole (h) states at energies $\varepsilon_{e(h)}$ of the configuration space sectors $N_{\pm} = n \pm 1$ for couple of the interacting magnetic cations (see. Fig.1):

$$\hat{H}_s = \sum_{i \neq j} J_{ij} \left(\hat{S}_{i n_0} \hat{S}_{j n_0} - \frac{1}{4} \hat{n}_{i n_0}^{(e)} \hat{n}_{j n_0}^{(h)} \right),$$

$$J_{ij} = \sum_{he} \frac{J_{ij}(h, n_0, e)}{(2S_h + 1)(2S_{n_0} + 1)} \quad (1)$$

where $J_{ij}(h, n_0, e) = 2 \left(t_{ij}^{n_0 h, n_0 e} \right)^2 / \Delta_{n_0 h e}$ and $\Delta_{n_0 h e} = \varepsilon_e + \varepsilon_h - 2\varepsilon_{n_0}$. All definitions of the multielectron spin $\hat{S}_{i n_0}$ and number of quasiparticles $\hat{n}_{i n_0}^{(e)}$ operators are in the Appendix. The second contribution in Eq.(1) differs from the generally accepted method of writing the superexchange interaction and coincides with the usual form $\frac{1}{4} \hat{n}_i \hat{n}_j$ for half-filled shells, where there is electron-hole symmetry. The superexchange interaction parameter J_{ij} in Eq.(1) is additive for all electronic $|e\rangle$ and hole $|h\rangle$ states in sectors N_{\pm} in Fig.1 and one is obtained in second order of cell perturbation theory over the interband contribution $\delta\hat{H}_1$ to the total Hamiltonian \hat{H}_1 of electron interatomic hopping:

interaction. The total multielectron Hamiltonian in the representation of the Hubbard operators³¹ looks like $\hat{H} = \hat{H}_0 + \hat{H}_1$, where \hat{H}_0 contains all multielectron states of the involved d^n and $d^{n\pm 1}$ configurations, and \hat{H}_1 described all interatomic single electron hoppings (kinetic

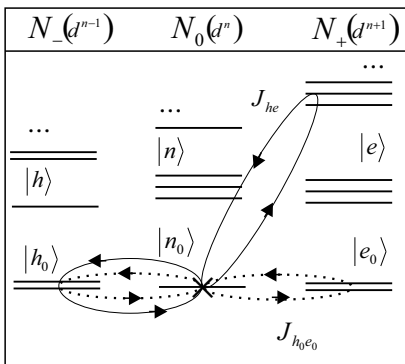


FIG. 1. The scheme of the superexchange interaction illustrating property of its additivity over virtual electron excitations involving all ground states $J_{h_0e_0}$ (dotted line, we call this contribution the main exchange loop) and the excited electronic d^{n+1} contribution J_{h_0e} (solid line, called the excited exchange loop).

energy):

$$\hat{H}_0 = \sum_i \left\{ \sum_h (\varepsilon_h - N_- \mu) X_i^{hh} + \sum_n (\varepsilon_n - N_0 \mu) X_i^{nn} + \sum_e (\varepsilon_e - N_+ \mu) X_i^{ee} \right\} \quad (3)$$

$$\hat{H}_1 = \sum_{ij} \sum_{rr'} t_{ij}^{rr'} X_i^r + X_j^{r'} \quad (4)$$

for the material with magnetic cations in arbitrary d^n electron configuration. Any Hubbard operator $X_i^r = |p\rangle \langle q|$ constructed in the full and orthogonal set of eigenstates $|p\rangle$ is numerated by a pair of indexes which denotes the initial state $|q\rangle$ and the final state $|p\rangle$ of the excitation.^{31,32} It is more convenient to numerate each excitation by single vector index $r = (p, q)$ (so called root vector³³ that plays a role of the quasiparticle band index). Here, electronic creation operators for vector indexes $r = (n, h)$ or $r = (e, n)$ excitations in Eq.(2) are denoted by $\beta_{i\sigma}^+$ ($N_- \rightarrow N_0$) and $\alpha_{i\sigma}^+$ ($N_0 \rightarrow N_+$) respectively. The hopping matrix element in Eq.(4) is

$$t_{fg}^{rr'} = \sum_{\lambda\lambda'} t_{fg}^{\lambda\lambda'} \sum_{\sigma} [\gamma_{\lambda\sigma}^*(r) \gamma_{\lambda'\sigma}(r') + \gamma_{\lambda'\sigma}^*(r) \gamma_{\lambda\sigma}(r')] \quad (5)$$

and

$$\gamma_{\lambda\sigma}(r) = \langle e | c_{i\lambda\sigma}^+ | n \rangle \times \delta_{S_{ie}, S_{in\pm|\sigma|}} \times \delta_{M_e, M_n+\sigma} \quad (6)$$

where a root vectors r and r' run over on all possible quasiparticle excitations (e, n) and (n, h) between many-electron states $|n\rangle$ and $|e(h)\rangle$ with the energies ε_n and $\varepsilon_{e(h)}$ in the sectors N_0 and N_{\pm} of configuration space (Fig.1). These quasiparticle excitations are described by nondiagonal elements $t_{fg}^{rr'} = t_{ij}^{nh,ne}$. In the conventional Hubbard model there is only one such element

corresponding to the excitations between lower and upper Hubbard bands. Using the results of Appendix (see Eq.(A.12)), we can represent the exchange parameter for a pair of interacting spins $S_{in_0} = S_{jn_0}$ in the form of Eq.(7):

$$J_{ij} = J_{ij}^{AFM} + J_{ij}^{FM}. \quad (7)$$

This equality and its relationship with the spin $S_{h(e)}$ at the states $|h(e)\rangle$ was obtained in the works^{5,19} for iron borate and also was firstly briefly mentioned in the works.^{34,35} The virtual electron interband (n_0, e) and (n_0, h) hoppings correspond to only one of contributions in the sum $J_{ij} = \sum_{he} J_{ij}(h, n_0, e)$, and any contribution $J_{he} = \sum_{ij} J_{ij}(h, n_0, e)$ can be represented by a double loop or the so-called exchange loop, marked by the same line (solid or dashed). In Fig.1 the contributions J_{he} is illustrated by double exchange loops with the arrows which connect the ground state of the magnetic ions $|n_0\rangle$ with all ground $|h_0(e_0)\rangle$ and excited $|h(e)\rangle$ states.

III. RULES FOR A SIGN OF DIFFERENT CONTRIBUTIONS TO THE SUPEREXCHANGE

The new result of this paper is the classification of different contributions by the relation between spins S_h and S_e . If in exchange loop $S_h = S_e \pm 1$ it will be FM contribution, in the other case $S_h = S_e$ it is AFM contribution. These two relations exhaust all possible interrelations between spins for all nonzero contributions, i.e. in any other case, the contribution to superexchange from this pair of states $|h\rangle$ and $|e\rangle$ is simply not available. The sign of the total exchange interaction (FM or AFM) depends on a relationship between relative magnitudes of the contributions. The main difficulty is a great number of excited states in N_{\pm} sectors of the configuration space. Due to the smallest denominator $\Delta_{n_0h_0e_0}$ in the superexchange (1), the main exchange loop involving ground $|h_0(e_0)\rangle$ states can form a dominant $J_{h_0e_0}$ contribution. However, the contributions J_{he} from the excited states $|h(e)\rangle$ in N_{\pm} sectors can compete with the main exchange loop due to the dominant nominator, if the excited exchange loop occurs by overlapping of states with e_g symmetry, and the main exchange loop is formed by π bonding despite not the smallest denominator Δ_{n_0he} in Eq.(1). The problem is that without complicated numeric calculation taking into account all hopping integrals (4), it is difficult to obtain the final answer about the magnitude and sign of the superexchange interaction. For example, such numerical calculations have been carried out for La_2CuO_4 with a configuration d^9 , where a number of the contributions exceeds ten ones.^{36,37} We will give a qualitative criterion that takes into account both factors in the case both σ or π overlapping in the

Hamiltonian (2) (where $t_{ij}^{el, hn}$ hopping is obtained by the mapping of the multiband p-d model, which includes integral for σ or π overlapping), and the energy gap Δ_{nhe} in the arbitrary exchange loop J_{he} . The minimal gap $\Delta_{n_0 h_0 e_0}$ just coincide with a dielectric gap E_g in the oxide materials. After comparing calculated sign of the superexchange constant for magnetic ions in the electron configurations $d^2 - d^8$ with experimental data, we found that in most cases there is no need to sum over all possible virtual hoppings (or exchange loops), it is enough to establish the criterion in form:

1. For the σ overlapping e_g states corresponding to contribution $J_{h_0 e_0}$, the sign of superexchange is controlled by the virtual electron excitations with participate of the ground $|h_0(e_0)\rangle$ states and minimal magnitude of the energy gap $\Delta_{n_0 h_0 e_0} \sim E_g$. These excitations involved to the main exchange loop is pictured in Fig.1 by a dashed line.

2. In the case of π overlapping t_{2g} states for the virtual electron excitations involving only the ground $|h_0(e_0)\rangle$ states the sign of superexchange is controlled by not the main exchange loop, but the virtual electron excitations (exchange loop) involving the excited states with the σ overlapping e_g states. These virtual excitations are pictured in Fig.1 by solid line. If such exchange loops is absent, the sign of superexchange is controlled still by the main loop with the π overlapping.

Here, the σ overlapping have the priority. Indeed, the superexchange interaction is proportional to the fourth degree of the overlapping integral $I_{\sigma(\pi)} = \rho(|\Delta R|) \chi_{\sigma(\pi)}$ between the electron states of the anion and the magnetic cation, where the radial part $\rho(|\Delta R|)$ depends only on the anion-cation distance ΔR , and the angular part $\chi_{\sigma(\pi)}$ depends on the angular distribution of the anions. The squared ratio $(I_{\pi}/I_{\sigma})^2$ of the overlapping integrals for e_g and t_{2g} states involved in the superexchange through

σ and π coupling in the same octahedral complexes is the following relation: $(I_{\pi}/I_{\sigma})^2 = (\chi_{\pi}/\chi_{\sigma})^2 = 1/3$. Thus the fourth degree gives ratio of matrix elements ~ 0.1 , i.e., competition between the contributions with a participation of virtual t_{2g} electron hopping and the one through σ coupling is possible, when the denominator energy Δ_{nhe} for excited loop J_{he} is no more than 9 times higher in energy than the main loop energy $\Delta_{n_0 h_0 e_0}$. Otherwise the σ type contribution from exchange loop is dominant. In case of several competing contributions simple calculations of the multielectron energies below and above the spin crossover at the high pressure³⁸ can be used to compare energy denominators of the AFM and FM contributions given by Eq.(7). Some examples will be given in the next section for oxide materials with d^7 and d^5 cations.

IV. SUPEREXCHANGE IN OXIDES WITH CATIONS IN d^7 AND d^5 CONFIGURATIONS

Let us show, using the example of oxide materials CoO and Ni₂O₃ with Ni³⁺, Co²⁺ cations in the d^7 electron configuration under high pressure, how our rules work. The energy of the neutral $|n\rangle$ (d^7) states and electronic $|e\rangle$ (d^8) and hole $|h\rangle$ (d^6) states at the ambient pressure are shown in Fig.2(a). From the main exchange loop with π overlapping our rules results in the FM sign of the contribution $J_{5T, 3A}$. Competing AFM contribution is the exchange loop $J_{3T, 3T}$ with the excited states $|^3T_{1,2}\rangle$ and σ overlapping. Below we will check our rules by direct calculation for the main exchange loop. To derive the FM contribution $J_{5T, 3A}$ using angular momentum addition rules, we introduce the creation operators $\beta_{i\sigma}^+$ (n_0, h_0) for $N_- \leftrightarrow N_0$ hole quasiparticles by Eq.(7) and $\alpha_{i\sigma}^+$ (e_0, n_0) for $N_0 \leftrightarrow N_+$ electron quasiparticles by Eq.(8).⁵

$$\begin{aligned} -\beta_{i\uparrow}^+ &= \sqrt{\frac{1}{5}}X_i^{\frac{3}{2},1} + \sqrt{\frac{2}{5}}X_i^{\frac{1}{2},0} + \sqrt{\frac{3}{5}}X_i^{-\frac{1}{2},-1} + \sqrt{\frac{4}{5}}X_i^{-\frac{3}{2},-2}, \beta_{i\downarrow}^+ = \sqrt{\frac{4}{5}}X_i^{\frac{3}{2},2} + \sqrt{\frac{3}{5}}X_i^{\frac{1}{2},1} + \sqrt{\frac{2}{5}}X_i^{-\frac{1}{2},0} + \sqrt{\frac{1}{5}}X_i^{-\frac{3}{2},-1} \\ -\alpha_{i\uparrow}^+ ({}^3A_2, {}^4T) &= \sqrt{\frac{1}{4}}X_i^{1,\frac{1}{2}} + \sqrt{\frac{1}{2}}X_i^{0,-\frac{1}{2}} + \sqrt{\frac{3}{4}}X_i^{-1,-\frac{3}{2}}, \alpha_{i\downarrow}^+ ({}^3A_2, {}^4T) = \sqrt{\frac{3}{4}}X_i^{1,\frac{3}{2}} + \sqrt{\frac{1}{2}}X_i^{0,\frac{1}{2}} + \sqrt{\frac{1}{4}}X_i^{-1,-\frac{1}{2}} \end{aligned} \quad (8)$$

Working further in framework of the cell perturbation theory, we obtain in the second order the FM contribution $J_{5T, 3A}$ from the main exchange loop in Fig.2 with the π overlapping:

$$J_{5T, 3A} = - \sum_{i \neq j} \frac{J_{ij} ({}^5T, {}^3A)}{(5)(3/2)} \left(\hat{S}_{in_0} \hat{S}_{jn_0} + \frac{1}{4} \hat{n}_{in_0}^{(e)} \hat{n}_{jn_0}^{(h)} \right) \quad (9)$$

where $S_{in_0} = \frac{3}{2}$, $\hat{S}_{in_0}^+ = -5\beta_{i\uparrow}^+ \beta_{i\downarrow} = -4\alpha_{i\downarrow} \alpha_{i\uparrow}^+$, $\hat{S}_{in_0}^z = -5 \sum_{\sigma} \eta(\sigma) \beta_{i\sigma}^+ \beta_{i\sigma} = -4 \sum_{\sigma} \eta(\sigma) \alpha_{i\sigma} \alpha_{i\sigma}^+$, and also $\hat{n}_{in_0}^{(e)} =$

$5 \sum_{\sigma} \beta_{i\sigma}^+ \beta_{i\sigma}$ and $\hat{n}_{jn_0}^{(h)} = 4 \sum_{\sigma} \alpha_{j\sigma} \alpha_{j\sigma}^+$ are the number of electron and hole quasiparticles involved in the superexchange interaction. According to a second point of the criterion the FM contribution competes with the AFM $J_{3T, 3T}$ contribution:

$$J_{3T, 3T} = \sum_{i \neq j} \frac{J_{ij} ({}^3T, {}^3T)}{(3)(3/2)} \left(\hat{S}_{in_0} \hat{S}_{jn_0} - \frac{1}{4} \hat{n}_{in_0}^{(e)} \hat{n}_{jn_0}^{(h)} \right) \quad (10)$$

from the virtual α hoppings of e_g electrons with participa-

tion of the states $|^3T_{1,2}\rangle$ and σ overlapping (see Fig.2(a)). Similarly to Eqs.(7) and (8), new $\alpha'_{i\sigma}^+$ and $\beta'_{i\sigma}^+$ quasipar-

ticles involved in this superexchange are given by the expression:

$$\begin{aligned} \beta'_{i\uparrow}^+(4T, 3T) &= X_i^{\frac{3}{2},1} + \sqrt{\frac{2}{3}}X_i^{\frac{1}{2},0} + \sqrt{\frac{1}{3}}X_i^{-\frac{1}{2},-1}, \beta'_{i\downarrow}^+(4T, 3T) = \sqrt{\frac{1}{3}}X_i^{\frac{1}{2},1} + \sqrt{\frac{2}{3}}X_i^{-\frac{1}{2},0} + X_i^{-\frac{3}{2},-1}; \\ -\alpha'_{i\uparrow}^+(3T, 4T) &= \sqrt{\frac{1}{4}}X_i^{1,\frac{1}{2}} + \sqrt{\frac{2}{4}}X_i^{0,-\frac{1}{2}} + \sqrt{\frac{3}{4}}X_i^{-1,-\frac{3}{2}}, \alpha'_{i\downarrow}^+(3T, 4T) = \sqrt{\frac{3}{4}}X_i^{1,\frac{3}{2}} + \sqrt{\frac{1}{2}}X_i^{0,\frac{1}{2}} + X_i^{-1,-\frac{1}{2}} \end{aligned} \quad (11)$$

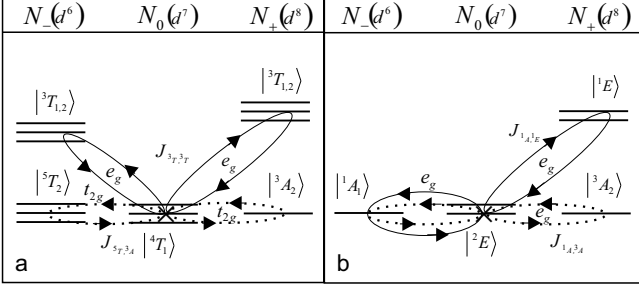


FIG. 2. Scheme of the 180° superexchange interaction in CoO: (a) at the ambient pressure, where AFM interaction is controlled by the contribution from the exchange loop $J_{3T,3T}$ with the excited states $|^3T_{1,2}\rangle$ and σ overlapping. The contribution $J_{5T,3A}$ from the main exchange loop $J_{1A,3A}$ with π overlapping is showed by a dotted line; (b) under high pressure, where FM character is controlled by the main exchange loop $J_{1A,3A}$ with the σ overlapping. The AFM contribution from the exchange loop $J_{1A,1E}$ with participation of excited states $|^1E\rangle$ has a large denominator.

Here: $\hat{S}_{in_0}^+ = 3\beta'_{i\uparrow}^+\beta'_{i\downarrow} = -4\alpha'_{i\downarrow}\alpha'_{i\uparrow}$, $\hat{S}_{in_0}^z = 3\sum_{\sigma}\eta(\sigma)\beta'_{i\sigma}^+\beta'_{i\sigma} = -4\sum_{\sigma}\eta(\sigma)\alpha'_{i\sigma}\alpha'_{i\sigma}$ and $\hat{n}_{in_0}^{(e)} = 3\sum_{\sigma}\beta'_{i\sigma}^+\beta'_{i\sigma}, \hat{n}_{in_0}^{(h)} = 4\sum_{\sigma}\alpha'_{i\sigma}\alpha'_{i\sigma}$. Calculation of energies of the different states below and above spin crossover allows us to obtain the energy denominators for the different contributions to superexchange interaction. For the main exchange loop $J_{5T,3A}$ in Fig.2(a) the value $\Delta_{n_0he} = U - J_H$, where U is the intra-atomic Coulomb matrix element (Hubbard parameter) and J_H is the Hund exchange coupling, both U and J_H are positive. For the contribution from exchange loop $J_{3T,3T}$, $\Delta_{n_0he} = \varepsilon_e + \varepsilon_h - 2\varepsilon_{n_0} = U + J_H$. At the typical magnitudes $U = 6eV$ and $J_H = 1eV$ the ration of denominators is $5/8$, and the ratio of numerators is $9/1$. It proves the dominant AFM contribution below spin crossover. With increasing pressure there is the spin crossover in configuration d^7 . The pressure enter in the crystal field parameter $10Dq$ that linearly increases with the pressure: below spin crossover at the ambient pressure when $10Dq < 2J_H$ the cation Co^{3+} is at the HS state, and $|n_0\rangle = |^4T_1\rangle$, $|h_0\rangle = |^5T_2\rangle$, $|e_0\rangle = |^3A_1\rangle$ (see Fig.2(a)).

Above spin crossover at $10Dq > 2J_H$ the cation Co^{3+} is at the LS state $|n_0\rangle = |^2E\rangle$, and $|h_0\rangle = |^1A\rangle$ (see Fig.2(b)).³⁸ Thus, the ground $|n_0\rangle$ and hole $|h_0\rangle$ states the superexchange interactions in the cobalt monoxide under high pressure is changed. The main exchange loop $J_{1A,3A}$ with the σ overlapping should be FM according our rules.

$$J_{1A,3A} = -\sum_{i\neq j} \frac{J_{ij}(^1A, ^3A)}{2} \left(\hat{S}_{in_0}\hat{S}_{jn_0} + \frac{1}{4}\hat{n}_{in_0}^{(e)}\hat{n}_{jn_0}^{(h)} \right) \quad (12)$$

The AFM contribution from the exchange loop with the excited states has the large denominator than the FM one (Fig.2b).

$$J_{1A,1E} = \sum_{i\neq j} \frac{J_{ij}(^1A, ^1E)}{2} \left(\hat{S}_{in_0}\hat{S}_{jn_0} - \frac{1}{4}\hat{n}_{in_0}^{(e)}\hat{n}_{jn_0}^{(h)} \right) \quad (13)$$

These conclusions can be obtained analogously to the previous Eq.(9) and Eq.(10), starting from building operators $\beta_{i\sigma}^+, \alpha_{i\sigma}^+$ and $\beta'_{i\sigma}^+, \alpha'_{i\sigma}^+$ of the quasiparticles and finishing with derivation of the Eqs.(12) and (13). We have to compare the energy denominators. For FM contribution $J_{1A,3A}$, the energy $\Delta_{1A,3A} = \varepsilon(^1A, d^6) + \varepsilon(^3A, d^8) - \varepsilon(^2E, d^7) = U - J_H$ and $\Delta_{1A,1E} = U$. Taking into account that all contributions have the same σ bonding, we came to conclusion that resulting interaction in the LS state for materials with the cations in d^7 configuration will be FM.

Let's compare our conclusions with the results for iron borate $FeBO_3$ at the high pressure. Under pressure $P \sim 60GPa$ in the iron borate with cations Fe^{3+} in the configuration d^5 the spin crossover $|^6A_1\rangle \rightarrow |^2T_2\rangle$ occurs at $10Dq = 3J_H$. Given above criterion tells us that the sign of the exchange interaction in iron borate is changed from AFM to FM with increasing pressure in agreement with direct calculations.¹⁹ This conclusion is also valid for another oxide materials with cations in the configuration d^5 and octahedral environment.

At the ambient pressure FM contributions from the exchange loops are missing (Fig.3(a)). The AFM superexchange interaction is caused by the contribution $J_{5E,5E}$ from the σ bonding exchange loop with the excited $|e\rangle$ states. The calculation of the energy denominator is

TABLE I. The examples of transition metals oxides with calculated sign of 180° superexchange interactions (in 3 and 5 columns), and also the magnetic ordering below and above the spin crossover (in 4 and 6 columns). The notations (ex) and (gr) indicates the nature of the main contribution to the superexchange: (ex) is the exchange loop involving excited states, (gr) is the main exchange loop.

Cation and electron configuration	Oxides	Superexchange below spin crossover	Ambient pressure (experiment)	Superexchange above spin crossover	High pressure (experiment)
d^2 , Cr^{4+} , $S_{n_0} = 1$	CrO_2	$J_{2T,4A}^{FM}(\text{gr})$	FM, $T_C = 90K$	no crossover, $J_{2T,4A}^{FM}(\text{gr})$, $S_{n_0} = 1$	FM up to $P=56\text{GPa}$, ³⁹
d^3 , Cr^{3+} , $S_{n_0} = \frac{3}{2}$	LaCrO_3	$J_{3T,3T}^{AFM}(\text{ex})$	AFM, $T_N = 298K$ ⁴⁰	no crossover $J_{3T,3T}^{AFM}(\text{gr})$, $S_{n_0} = \frac{3}{2}$	AFM, T_N increases with a pressure up to $380K$ at $P=6.5\text{GPa}$ ⁴⁰
d^4 , Fe^{4+} , Mn^{3+} , $S_{n_0} = 2$	LaMnO_3	$J_{4A,6A}^{FM}(\text{gr})$	AFM, with FM planes $T_N = 140K$, ⁴¹	crossover is expected to the LS state, $J_{4A,2T}^{FM}(\text{gr})$, $S_{n_0} = 1$	AFM, $T_N = 152K$ at the pressure $P=2\text{GPa}$. FM above the spin crossover is predicted.
d^5 , Fe^{3+} , Mn^{2+} $S_{n_0} = \frac{5}{2}$	FeBO_3 , (Fe_2O_3 , MnO)	$J_{5E,5E}^{AFM}(\text{ex})$	AFM, $T_N = 348K$ ⁴²	spin crossover, $J_{3T,1A}^{FM}(\text{gr})$ $S_{n_0} = \frac{1}{2}$	$T_{N(C)} = 50K^*$, at $P=49\text{GPa}$, FM above the spin crossover is predicted.
d^6 , Fe^{2+} , Co^{3+} $S_{n_0} = 2$	$\text{Mg}_{1-x}\text{Fe}_x\text{O}$, (LaCoO_3)	$J_{4T,4T}^{AFM}(\text{ex})$	AFM, $T_N = 37K$ ⁴³	spin crossover to nonmagnetic state with $S_{n_0} = 0$	non magnetic above $P=55\text{GPa}$ ^{43,44}
d^7 , Co^{2+} , Ni^{3+} , $S_{n_0} = \frac{3}{2}$	CoO , (La_2CoO_4 , LaNiO_3)	$J_{3T,3T}^{AFM}(\text{ex})$	AFM, $T_N = 290K$ ⁴⁵	spin crossover is expected, $J_{1A,3A}^{FM}(\text{gr})$, $S_{n_0} = \frac{1}{2}$	spin crossover observed at $P=80-90\text{GPa}$ ^{46,47}
d^8 , Ni^{2+} , Cu^{3+} $S_{n_0} = 1$	NiO	$J_{2E,2E}^{AFM}(\text{ex})$	AFM, $T_N = 525K$	no spin crossover, $J_{2E,2E}^{AFM}$, $S_{n_0} = 1$	no spin crossover observed up to $P=220\text{GPa}$ ^{7,48}

*The critical temperature $T_{N(C)}$ of magnetic ordering in iron borate FeBO_3 at the higher pressure was measured by Mossbauer spectroscopy,^{7,42} however, this method cannot distinguish the nature (FM or AFM) of the magnetic ordering. Up to now there is no experimental data on the magnetic ordering in the LS state of FeBO_3 or any other materials with d^5 cations.

$\Delta_{5E^5T} = U - 10Dq + 4J_H$. Thus, the AFM exchange interaction at the ambient pressure may be estimated as $J_{5E^5T} \approx t_\sigma^2/(U + J_H)$. Crystal field increases with pressure, and at the critical pressure $10Dq(P_c) = 3J_H$ there is spin crossover $|^6A_1\rangle \rightarrow |^2T_2\rangle$. Above the spin crossover, the nature of the FM superexchange interaction is obtained from the competition of FM($J_{3T,1A}$) and AFM ($J_{1T,1A}$) loops with the same type of π overlapping, where the FM contribution prevails (see Fig.3(b) due to the smaller magnitude of the energy gap Δ_{n_0he} . We can estimate the competing FM and AFM by calculation of their energy denominators. For the main FM exchange loop (dotted lines in Fig.3(b) the energy $\Delta_{5T^1A} \approx U - J_H$,

and for the excited AFM loop (solid lines in Fig.3(b) the energy $\Delta_{1T^1A} \approx U$. That is why the FM contribution dominates. Nevertheless the AFM one strongly reduced the total FM superexchange interaction, that can be estimated as

$$J_{FM} = J_{5E^5T} + J_{5E^5T} \approx \frac{t_\pi^2}{U - J_H} - \frac{t_\pi^2}{U} = \frac{t_\pi^2}{U - J_H} \frac{J_H}{U} \quad (14)$$

Thus, spin crossover in oxide materials with d^5 cations not only changes the sign of exchange interaction, but also reduces its amplitude by the factor $J_H/U \ll 1$.

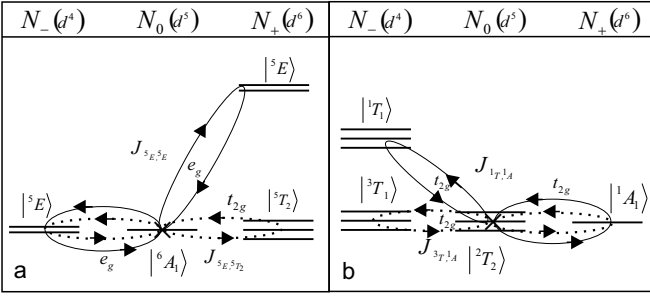


FIG. 3. Scheme of the 180° superexchange interaction in FeBO_3 : (a) at the ambient pressure, where the main exchange loop $J_{5E,5T_2}$ has a zero contribution because of zero overlapping, and the σ overlapping exchange loops $J_{5E,5E}$ result in AFM contribution only; (b) under high pressure, where both contributions $J_{3T,1A}$ (FM) and $J_{1T,1A}$ (AFM) are proportional to π overlapping. The FM contribution $J_{3T,1A}$ dominates.

V. SUPEREXCHANGE IN OXIDES WITH CATIONS IN OTHER ELECTRON CONFIGURATIONS

Now, we can obtain the nature (FM or AFM) of the superexchange interaction for oxide materials with d^2 - d^8 cations under pressure, below and above the spin crossover in Tab.1, and also compare one with experimental data, where it is possible. In the oxide materials with another d^n ions, where $n = 2, 3$, spin crossover is not possible, and ground states $|^3T_1\rangle$ and $|^4A_2\rangle$ is stable under high pressure.

d^2 . Chromium dioxide CrO_2 , where chrome cation Cr^{4+} has configuration d^2 with spin $S_{n_0} = 1$, is the example of FM contribution $J_{2T,4A}$ from the main exchange loop involving the ground states of t_{2g} cation with the π overlapping at an arbitrarily pressure. FM ordering in chromium dioxide is known experimentally and persists in orthorhombic phase of the chromium dioxide up to $P=55\text{GPa}$.³⁹

d^3 . For chromium oxide LaCrO_3 with cations Cr^{3+} at the ground state $|^4A_2\rangle$ is stable under pressure, and the dominant AFM contribution is given by the exchange loop with the ground state $|h_0\rangle = |^3T\rangle$ in the hole configuration d^2 and the excited state $|n\rangle = |^3T\rangle$ in the electron d^4 configuration. Under high pressure when $10Dq(P) > 3J_H$ the crossover stabilizes the triplet $|n_0\rangle = |^3T\rangle$. The AFM sign of the exchange interaction does not change, but the same interaction $J_{3T,3T}$ is described by the main exchange loop and its value becomes larger.

d^4 . In manganite LaMnO_3 at the ambient pressure with cations Mn^{3+} at the ground HS state $|n_0\rangle = |^5E\rangle$, the σ overlapping main loop $J_{4A,6A}$ results in the FM interaction. Under high pressure $10Dq(P) > 3J_H$ when the cations Mn^{3+} are in the intermediate spin state $|n_0\rangle = |^3T\rangle$, and all superexchange interactions results from the π bonding. The main exchange loop provides

the FM interaction $J_{4A,2T}$, with the energy denominator $\Delta_{4A,2T} = U - J_H$, while exchange via excited states gives the AFM contribution $J_{2T,2T}$ with $\Delta_{2T,2T} = U + J_H$, and the total superexchange interaction has the FM sign. It should be emphasized that in this study we consider the crystals with cations in the octahedral oxygen environment. When we compare our conclusions about the FM interaction with the magnetic state of manganite, we find the disagreement with its AFM ordering at the ambient pressure. Nevertheless this AFM ordering consists of the FM ab planes that are AFM coupled. This disagreement is probably related to the dependence of the magnetic ordering on the type of orbital ordering in the oxide material with Jahn - Teller cations Mn^{3+} .^{49,50} With increasing pressure, the spin crossover in is accompanied by the transition of the cation Mn^{3+} from the HS Jahn - Teller state $|^5E\rangle$ to the state $|^3T\rangle$. Therefore, the orbital ordering with increasing pressure should disappear, and the FM nature of the superexchange will manifest itself (see Tab. 1).

d^6 . At the ambient pressure, in the wustite $\text{Mg}_x\text{Fe}_{1-x}\text{O}$ with cations Fe^{2+} in the configuration d^6 there is a competition of two different contributions $J_{4T,4T}^{AFM}$ with σ overlapping and $J_{6A,4T}^{FM}$ with π overlapping, and the AFM contribution dominates. At high pressures ($P = 55\text{GPa}$), the magnetic moment in the wustite is absent as well as in all other compounds with cations in configuration d^6 . The large class of such materials with $S_{n_0} = 0$ in the ground state is given by the perovskite based rare earth cobaltite LaCoO_3 , where La^{3+} is the 4f ion.

d^8 . For nickel monoxide NiO with cations Ni^{2+} in the configuration d^8 situation is similar to the configuration d^3 . There is no spin crossover in the neutral configuration d^8 and at the ambient pressure the AFM interaction $J_{2E,2E}^{AFM}$ involves the excited state $|h\rangle = |^2E\rangle$ in the hole configuration d^7 . Above the spin crossover in the hole configuration this state becomes the ground one $|h_0\rangle = |^2E\rangle$, and the same AFM interaction $J_{2E,2E}^{AFM}$ is given now by the main exchange loop. Thus, its value increases due to the spin crossover in the hole configuration d^7 . Summarizing our analysis we get together all our conclusions in Tab.1, and also compare them with experimental data, where it is possible.

VI. CONCLUSIONS

The sign of the partial contributions J_{he} to the total superexchange interaction is directly independent on the cation spin $S(d^n)$, but is controlled by the spin relation $S(d^{n-1}) = S(d^{n+1})$ (AFM interaction) or $S(d^{n-1}) = S(d^{n+1}) \pm 1$ (FM interaction) provided that $S(d^n) = S(d^{n\pm 1}) \pm 1/2$ (see Eqs.(A.12) and (A.14)). Indeed the chromium dioxide CrO_2 and nickel monoxide NiO ($S_{n_0} = 1$), or manganites LaMnO_3 and wustite $\text{Mg}_{1-x}\text{Fe}_x\text{O}$ ($S_{n_0} = 2$), can have FM and AFM interactions respectively. The main factor for the comparison

between the AFM and FM interactions is the type overlapping states involved by the contributions. The nature of the superexchange interaction with increasing pressure changes (AFM→FM) only in oxide materials with cations in d^5 (e.g. FeBO₃) and d^7 (e.g. CoO) configurations. Indeed spin crossover $|^4T_1\rangle \rightarrow |^2E\rangle$ with generating Jahn-Teller cations Co²⁺ (2E) in cobalt monoxide at $P > 43$ Gpa is accompanied by: (i) transformation of the cubic rock salt-type structure to mixed rhombohedrally distorted rock salt-type structure without significant volume change structure; (ii) a resistance drop by eight orders of magnitude at the room temperature ($43\text{Gpa} < P < 63\text{Gpa}$) while maintaining its semiconductor nature; (iii) Mott-Hubbard transition into the metal rock salt structure at more high pressure $P > 120\text{Gpa}$.^{46,47} We did not find any studies related to high pressure effects in oxides La₂CoO₄ ($S_{n_0} = 3/2$, $T_N = 275\text{K}$ at the ambient pressure⁵¹) and LaNiO_{3-x} (paramagnetic metal⁵² and ultrathin film AFM insulator⁵³ at the ambient pressure). Unlike the cobalt oxides LaSrCoO₄ and LaCoO₃, with Co³⁺,⁵⁴ the layered oxide La₂CoO₄ has not been studied under the high pressure. However, these oxide materials⁵⁵ isostructural to well-known high- T_C and colossal magnetoresistance materials could have interesting physical properties at the high pressure ($>43\text{Gpa}$) and magnetic field. On the one hand, the high- T_C superconductors: doped and nonstoichiometric cuprates⁵⁶ with the multimode Jahn-Teller ($^2a_1 + ^2b_1$) \otimes ($b_{1g} + a_{1g}$) effect⁵⁷ and iron based superconductors,⁵⁸ have also the spin $S_{n_0} = 1/2$ and on the other hand, pseudogap effects and colossal magnetoresistance are observed in the doped manganite La(Sr,Ba)MnO₃ also with the Jahn-Teller Mn³⁺ (5E) cations.⁵⁹ However, the cobalt oxide La₂CoO₄ at the high pressure is very likely different from

cuprate La₂CuO₄ at the ambient pressure in a sign of the superexchange interaction, despite the same cation spin 1/2. Indeed the interaction in nickel monoxide does not undergo any critical changes with increasing pressure, either in theory or experiment, up to 220 GPa.⁷ Note, in the oxide materials: CrO₂, NiO, La₂CuO₄ with the cations in the electron configurations d^3 , d^8 , d^9 the spin crossover under high pressure is impossible.

The results partially disagree with experimental data at the ambient pressure only for oxide materials with Jahn-Teller d^4 cations like LaMnO₃, where the FM ab planes have AFM ordering. With increasing pressure, the spin crossover in manganite LaMnO₃ is accompanied by the transition of the magnetic Jahn-Teller Mn³⁺ cation to the state $|^3T\rangle$. In according to our conclusions, the effects of orbital ordering should disappear, and the FM nature of the superexchange will manifest itself (see Tab.1). Indeed, below pressure 29 GPa the manganite is not metallic and consists of a dynamic mixture of distorted and undistorted MnO₆ octahedral.⁶⁰ Above pressure 32 Gpa, undoped manganite already shows metallic properties.

ACKNOWLEDGMENTS

We acknowledge the support of the Russian Science Foundation through Grant 18-12-00022.

Appendix: AFM and FM contributions to superexchange interaction

To derive Eqs.(1) and (6), we start from the Hamiltonian of the p-d model, where

$$\hat{H} = \hat{H}_d + \hat{H}_p + \hat{H}_{pd} + \hat{H}_{pp}$$

$$\begin{aligned} \hat{H}_d &= \sum_{i\lambda\sigma} \left[(\varepsilon_\lambda - \mu) d_{\lambda i\sigma}^+ d_{\lambda i\sigma} + \frac{U_d}{2} \hat{n}_{\lambda i}^\sigma \hat{n}_{\lambda i}^{-\sigma} + \frac{1}{2} \sum_{\lambda' \neq \lambda} \left(\sum_{\sigma'} V_{\lambda\lambda'} \hat{n}_{\lambda i}^\sigma \hat{n}_{\lambda' i}^{\sigma'} - J_H d_{\lambda i\sigma}^+ d_{\lambda i\sigma} d_{\lambda' i\sigma}^+ d_{\lambda' i\sigma} \right) \right], \\ \hat{H}_p &= \sum_{m\alpha\sigma} \left[(\varepsilon_\alpha - \mu) p_{\alpha m\sigma}^+ p_{\alpha m\sigma} + \frac{U_p}{2} \hat{n}_{\alpha m}^\sigma \hat{n}_{\alpha m}^{-\sigma} + \frac{1}{2} \sum_{\alpha' \neq \alpha, \sigma'} V_{\alpha\alpha'} \hat{n}_{\alpha m}^\sigma \hat{n}_{\alpha' m}^{\sigma'} \right], \\ \hat{H}_{pd} &= \sum_{mi} \sum_{\alpha\lambda\sigma} \left[t_{im}^{\lambda\alpha} (p_{\alpha m\sigma}^+ d_{\lambda i\sigma} + h.c.) + \frac{V_{im}^{pd}}{2} \sum_{\sigma'} \hat{n}_{\alpha m}^\sigma \hat{n}_{\lambda i}^{\sigma'} \right], \quad \hat{H}_{pp} = \sum_{mn} \sum_{\alpha\beta\sigma} t_{mn}^{\alpha\beta} (p_{\alpha m\sigma}^+ p_{\beta n\sigma} + h.c.). \end{aligned} \quad (\text{A.1})$$

Here, $n_{\lambda i}^\sigma = d_{\lambda i\sigma}^+ d_{\lambda i\sigma}$, $n_{\alpha m}^\sigma = p_{\alpha m\sigma}^+ p_{\alpha m\sigma}$, where the indices $i(j)$ and $m(n)$ run over all positions $d_\lambda = d_{x^2-y^2}, d_{3z^2-z^2}, d_{xy}, d_{xz}, d_{yz}$ and $p_\alpha = p_x, p_y, p_z$ localized one electron states with energies ε_λ and ε_α ; $t_{im}^{\lambda\alpha}$ and $t_{mn}^{\alpha\beta}$ the hopping matrix elements; U_d , U_p and J_H are one site Coulomb interactions and the Hund exchange interaction, V_{im}^{pd} is the energy of repulsion of cation and

ion electrons. A correct transition from the Hamiltonian (A.1) of the p-d model to the Hamiltonian (3) in the multielectron representation of the Hubbard operators is possible when constructing well localized Wannier cell oxygen states $|p_{\lambda i\sigma}^+\rangle$. Although, there is no general derivation of the canonical transformation $|p_{\lambda i\sigma}^+\rangle \leftrightarrow |p_{\alpha m\sigma}^+\rangle$ for arbitrary lattice symmetry, we assume that the canonical representation does exist and that the Wannier cell

oxygen functions are sufficiently localized.^{61–63} In the multielectron representation the one-electron $p_{\lambda i \sigma}^+$ and $d_{\lambda i \sigma}^+$ operators can be written as a superposition of the Hubbard operators that describe one electron excitations from the LS and HS partner states $|h(e)\rangle$ with spin $S_{e(h)} = S_n \pm 1/2$ to the neutral state $|n\rangle$:

$$c_{\lambda i \sigma}^+ = \sum_n \left[\sum_e \gamma_\lambda(ne) \alpha_{i\sigma}^+(ne) + \sum_h \gamma_\lambda(nh) \beta_{i\sigma}^+(nh) \right], \quad (\text{A.2})$$

where the new operators $\alpha_{i\sigma}^+(en)$ and $\beta_{i\sigma}^+(nh)$ are notations for the electron addition to the ground state $N_0 \rightarrow N_+$, and to the hole state $N_- \rightarrow N_0$, respectively. Calculation of the matrix elements in Eq.(5) in agreement with the rules of addition of angular momentums results in the following relations:

$$\alpha_{i\sigma}^+(en) = \begin{cases} \eta(\sigma) \sum_{-M_e}^{M_e} \sqrt{\frac{S_n - \eta(\sigma)M_e + \frac{1}{2}}{2S_n + 1}} X_i^{M_e, M_n = M_e - \sigma} \\ \sum_{-M_e}^{M_e} \sqrt{\frac{S_n + \eta(\sigma)M_e + \frac{1}{2}}{2S_n + 1}} X_i^{M_e, M_n = M_e - \sigma} \end{cases} \quad (\text{A.3})$$

and

$$\beta_{i\sigma}^+(nh) = \begin{cases} \eta(\sigma) \sum_{-M_n}^{M_n} \sqrt{\frac{S_h - \eta(\sigma)M_n + \frac{1}{2}}{2S_h + 1}} X_i^{M_n, M_h = M_n - \sigma} \\ \sum_{-M_n}^{M_n} \sqrt{\frac{S_h + \eta(\sigma)M_n + \frac{1}{2}}{2S_h + 1}} X_i^{M_n, M_h = M_n - \sigma} \end{cases} \quad (\text{A.4})$$

where top and below lines are for $S_e = S_n - |\sigma|$ and $S_e = S_n + |\sigma|$ respectively. The superexchange interaction appears in the second order of the cell perturbation theory with respect to the hopping processes \hat{H}_1 in Eq.(3), which corresponds to virtual excitations through the dielectric gap into the conduction band and back

to valence band. These quasiparticle excitations correspond to the electron-hole excitations and are described by off-diagonal elements with root vectors $r = (h, n)$ and (n, e) . To highlight these contributions, we use a set of projection operators P_h and P_e , that generalized the Hubbard model analysis²⁶ to the Mott-Hubbard approach with an arbitrary quasiparticle spectrum, where $P_h = \left(X_i^{hh} + \sum_n X_i^{nn} \right) \left(X_j^{hh} + \sum_{n'} X_j^{n'n'} \right)$ and $P_e = X_i^{ee} + X_j^{e'e'} - X_i^{ee} \sum_{e'} X_j^{e'e'}$ with $1 \leq h \leq N_h$, $1 \leq n \leq N_n$ and $1 \leq e(e') \leq N_e$. These operators satisfies the relations $\left(\sum_{h=1}^{N_h} P_h + \sum_{e=1}^{N_e} P_e \right) = 1$ and $P_h P_e = 0$, $P_h P_{h'} = \delta_{hh'} P_h$, $P_e P_{e'} = \delta_{ee'} P_e$. We introduce the Hamiltonian of the exchange coupled (i, j) -pairs: $\hat{h}_{ij} = \left(\hat{h}_0 + \hat{h}_1^{in} \right) + \hat{h}_1^{out}$, where $\left(\hat{h}_0 + \hat{h}_1^{in} \right) = \sum_{hh'} P_h \hat{h}_{ij} P_{h'} + \sum_{ee'} P_e \hat{h}_{ij} P_{e'}$ and $\hat{h}_1^{out} = \left(\sum_h P_h \right) \hat{h}_{ij} \left(\sum_e P_e \right) + \left(\sum_e P_e \right) \hat{h}_{ij} \left(\sum_h P_h \right)$ is the intra- and interband contributions for Hamiltonian $\hat{H}_1 = \sum_{ij} \hat{h}_{ij}$ respectively. In the unitary transformation the Hamiltonian for (i, j) -pairs is equal to $\tilde{h}_{ij} = e^{\hat{G}} \hat{h}_{ij} e^{-\hat{G}}$, where \hat{G} satisfies the equation

$$\left(\sum_h P_h \right) \hat{h}_{ij} \left(\sum_e P_e \right) + \left(\sum_e P_e \right) \hat{h}_{ij} \left(\sum_h P_h \right) + \left[\hat{G}, \left(\sum_{hh'} P_h \hat{h}_{ij} P_{h'} + \sum_{ee'} P_e \hat{h}_{ij} P_{e'} \right) \right] = 0, \quad (\text{A.5})$$

and the transformed Hamiltonian \tilde{h}_{ij} in the second order of cell perturbation theory over interband hopping \hat{h}_1^{out} can be represented as

$$\tilde{h}_{ij} \approx \left(\sum_{hh'} P_h \hat{h}_{ij} P_{h'} + \sum_{ee'} P_e \hat{h}_{ij} P_{e'} \right) + \frac{1}{2} \left[\hat{G}, \left\{ \left(\sum_h P_h \right) \hat{h}_{ij} \left(\sum_e P_e \right) + \left(\sum_e P_e \right) \hat{h}_{ij} \left(\sum_h P_h \right) \right\} \right] \quad (\text{A.6})$$

where

$$\begin{aligned} \left(\sum_h P_h \right) \hat{h}_{ij} \left(\sum_e P_e \right) &= \sum_{n\sigma} \sum_{he} t_{ij}^{en, hn} \alpha_{i\sigma}^+(en) \beta_{j\sigma}(hn), \\ \left(\sum_e P_e \right) \hat{h}_{ij} \left(\sum_h P_h \right) &= \sum_{n\sigma} \sum_{he} t_{ij}^{ne, nh} \beta_{i\sigma}^+(nh) \alpha_{j\sigma}(ne) \end{aligned} \quad (\text{A.7})$$

and

$$\hat{G} = \sum_{nhe} \left[\frac{t_{ij}^{en, hn}}{\Delta_{nhe}} \sum_{\sigma} \alpha_{i\sigma}^+(en) \beta_{j\sigma}(hn) - \frac{t_{ij}^{ne, nh}}{\Delta_{n_0 he}} \sum_{\sigma} \beta_{i\sigma}^+(nh) \alpha_{j\sigma}(ne) \right] \quad (\text{A.8})$$

with the energy denominator is $\Delta_{nhe} = (\varepsilon_e + \varepsilon_h) - 2\varepsilon_n$. The effects of the ligand environment of magnetic ions are taken into account, due to the Wannier oxygen cell functions, as well as the exact diagonalization procedure when constructing the configuration space of the cell $|n\rangle$

and $|h(e)\rangle$ states with energies ε_n and $\varepsilon_{e(h)}$ respectively.

In agreement with the relations:

$$\begin{aligned}\hat{n}_{in\sigma}^{(e)} &= (2S_h + 1) \beta_{i\sigma}^{(t)+}(nh) \beta_{i\sigma}^{(t)}(hn), \\ n_{in\sigma}^{(h)} &= (2S_n + 1) \alpha_{i\sigma}^{(s)}(ne) \alpha_{i\sigma}^{(s)+}(en)\end{aligned}\quad (\text{A.9})$$

$$\begin{aligned}S_{in}^+ &= \begin{cases} (2S_h + 1) \beta_{i\uparrow}^+(nh) \beta_{i\downarrow}(hn) = (2S_n + 1) \alpha_{i\downarrow}(ne) \alpha_{i\uparrow}^+(en) , & S_n = S_h + |\sigma|; S_e = S_n + |\sigma| \\ - (2S_h + 1) \beta_{i\uparrow}^+(nh) \beta_{i\downarrow}(hn) = - (2S_n + 1) \alpha_{i\downarrow}(ne) \alpha_{i\uparrow}^+(en) , & S_n = S_h - |\sigma|; S_e = S_n - |\sigma| \end{cases} \\ \hat{S}_{in}^z &= \begin{cases} (2S_h + 1) \sum_{\sigma} \eta(\sigma) \beta_{i\sigma}^+ \beta_{i\sigma} = (2S_n + 1) \sum_{\sigma} \eta(\sigma) \alpha_{i\sigma} \alpha_{i\sigma}^+ , & S_n = S_h + |\sigma|; S_e = S_n + |\sigma| \\ - (2S_h + 1) \sum_{\sigma} \eta(\sigma) \beta_{i\sigma}^+ \beta_{i\sigma} = - (2S_n + 1) \sum_{\sigma} \eta(\sigma) \alpha_{i\sigma} \alpha_{i\sigma}^+ , & S_n = S_h - |\sigma|; S_e = S_n - |\sigma| \end{cases}\end{aligned}\quad (\text{A.10})$$

and assuming that the ground state $|n\rangle = |n_0\rangle$ is occupied at $T = 0K$, and the superexchange Hamiltonian takes the form:

$$\hat{H}_s = \sum_{i \neq j} \tilde{h}_{ij} = \sum_{i \neq j} \left\{ J_{ij}^- \hat{S}_{in_0} \hat{S}_{jn_0} - \frac{1}{4} J_{ij}^+ \hat{n}_{in_0}^{(e)} \hat{n}_{jn_0}^{(h)} \right\} \quad (\text{A.11})$$

where

$$\begin{aligned}J_{ij}^- &= \sum_{he}' \frac{J_{ij}(h, n_0, e)}{(2S_h + 1)(2S_{n_0} + 1)} \\ &\quad - \sum_{he}'' \frac{J_{ij}(h, n_0, e)}{(2S_h + 1)(2S_{n_0} + 1)},\end{aligned}\quad (\text{A.12})$$

and

$$\begin{aligned}J_{ij}^+ &= \sum_{he}' \frac{J_{ij}(h, n_0, e)}{(2S_h + 1)(2S_{n_0} + 1)} + \\ &\quad + \sum_{he}'' \frac{J_{ij}(h, n_0, e)}{(2S_h + 1)(2S_{n_0} + 1)}\end{aligned}\quad (\text{A.13})$$

and $\hat{n}_{in_0}^{(e)} = \sum_{\sigma} \hat{n}_{in_0\sigma}^{(e)}$, $\hat{n}_{in_0}^{(h)} = \sum_{\sigma} \hat{n}_{in_0\sigma}^{(h)}$. Since in the first contribution ($\sum_{he}' \dots$) the exchange loops are summed with $S_h = S_e$, and in the second one ($\sum_{he}'' \dots$), the exchange loops are with $S_h = S_e \pm 1$, so the superexchange \hat{H}_s contains all possible nonzero contributions, and the exchange constant J_{ij}^- in Eq.(A.11) is the sum of two AFM and FM contributions. Note, to obtain Eq.(A.12) for the same spins $S_{in_0} = S_{jn_0}$ at the different i and j cell of lattice we could use equality:

$$\begin{aligned}J_{ij} &= \sum_{he} J_{ij}(h, n_0, e) = J_{ij}^{AFM} + J_{ij}^{FM} = \\ &= 2 \sum_{he} \frac{\left(t_{ij}^{n_0h, n_0e}\right)^2 (\delta_{S_h, S_e} + \delta_{S_h, S_e \pm 1})}{\Delta_{n_0he}} \delta_{S_{n_0}, S_h + \sigma}\end{aligned}\quad (\text{A.14})$$

This is a simple but nonobvious conclusion, since the sign of the exchange parameter $J_{ij}^{AFM}(J_{ij}^{FM})$ becomes clear only after the spin correlators are derived from the operator structure of the Hamiltonian (2). Eqs.(A.12) and (A.13) extends the results of work⁵ to the oxide materials with arbitrary transition elements.

* gav@iph.krasn.ru

¹ P. W. Anderson, Phys. Rev. **115**, 2 (1959).

² Y. Tanabe and S. Sugano, J. Phys. Soc. Jpn **11**, 864 (1956).

³ J. H. Mentink and M. Eckstein, Phys. Rev. Lett. **113**, 057201 (2014).

⁴ A. M. Kalashnikova, A. V. Kimel, and R. V. Pisarev, Phys. Usp. **58**, 969980 (2015).

⁵ V. A. Gavrichkov, S. I. Polukeev, and S. G. Ovchinnikov, Phys. Rev. B **95**, 144424 (2017).

⁶ K. V. Lamonova, E. S. Zhitlukhina, R. Y. Babkin, S. M. Orel, S. G. Ovchinnikov, and Y. G. Pashkevich, J. Phys. Chem. **115**, 1359613604 (2011).

⁷ I. Lyubutin and A. Gavriluk, Phys. Usp. **52**, 9891017

(2009).

⁸ G. J. Halder, C. J. Kepert, B. J. Moubaraki, K. S. Murray, and J. D. Cashion, Science **298**, 1762 (2002).

⁹ S. Brooker and J. A. Kitchen, Dalton Trans. **36**, 7331 (2009).

¹⁰ S. Ohkoshi, K. Imoto, Y. Tsunobuchi, S. Takano, and H. Tokoro, Nat. Chem. **3**, 564 (2011).

¹¹ R. M. Wentzcovitch, J. F. Justo, Z. Wu, C. R. S. da Silva, D. A. Yuen, and D. Kohlstedt, Proceedings of the National Academy of Sciences of the United States of America **106**, 8447 (2009).

¹² H. Hsu, K. Umemoto, Z. Wu, and R. M. Wentzcovitch, Reviews in Mineralogy and Geochemistry **71**, 169 (2010).

- ¹³ J. Liu, J.-F. Lin, Z. Mao, and V. B. Prakapenka, *Am. Mineral.* **99**, 84 (2014).
- ¹⁴ R. Sinmyo, C. McCammon, and L. Dubrovinsky, *Am. Mineral.* **102**, 12631269 (2017).
- ¹⁵ A. Marbeuf, S. F. Matar, P. Negrier, L. Kabalan, J. F. Letard, and P. Guionneau, *Chem. Phys.* **420**, 25 (2013).
- ¹⁶ M. Nishino, K. Boukheddaden, Y. Konishi, and S. Miyashita, *Phys. Rev. Lett.* **98**, 247203 (2007).
- ¹⁷ S. Ovchinnikov and V. Zabluda, *JETP* **98**, 135 (2004).
- ¹⁸ T. Saha-Dasgupta and P. M. Oppeneer, *MRS Bulletin* **39**, 614 (2014).
- ¹⁹ V. A. Gavrichkov, S. I. Polukeev, and S. G. Ovchinnikov, *JETP* **127**, 713720 (2018).
- ²⁰ L. Bykova, L. Dubrovinsky, N. Dubrovinskaia, M. Bykov, C. McCammon, S. V. Ovsyannikov, H. P. Liermann, I. Kuppenko, A. I. Chumakov, R. Ruffer, M. Hanfland, and V. Prakapenka, *Nat. Comm.* **7**, 10661 (2016).
- ²¹ H. Eskes and J. H. Jefferson, *Phys. Rev. B* **48**, 9788 (1993).
- ²² Y. Ohta, T. Tohyama, and S. Maekawa, *Phys. Rev. Lett.* **66**, 1228 (1991).
- ²³ H. Eskes, G. A. Sawatzky, and L. F. Feiner, *Physica C* **160**, 424 (1989).
- ²⁴ E. B. Stechel and D. R. Jennison, *Phys. Rev. B* **38**, 4632 (1988).
- ²⁵ L. N. Bulayevskii, E. L. Nagaev, and D. I. Khomskii, *JETP* **27**, 836 (1968).
- ²⁶ K. A. Chao, J. Spalek, and A. M. Oles, *J. Phys. C: Solid State Physics* **10**, L271 (1977).
- ²⁷ J. B. Goodenough, *Magnetism and the Chemical Bond* (Interscience (Wiley), New York, 1963).
- ²⁸ J. Kanamori, *Magnetism, Vol. 1* (Academic Press Inc., New York, 1963).
- ²⁹ V. A. Gavrichkov, S. G. Ovchinnikov, A. A. Borisov, and E. G. Goryachev, *JETP* **91**, 369383 (2000).
- ³⁰ S. G. Ovchinnikov, V. A. Gavrichkov, M. M. Korshunov, and E. I. Shneyder, "Springer series in solid-state sciences, vol. 171," (2012) Chap. LDA+GTB method for band structure calculations in the strongly correlated materials, *Theoretical methods for Strongly Correlated Systems*, p. 147.
- ³¹ J. Hubbard, *Proc. Roy. Soc. A.* **277(1369)**, 237 (1964).
- ³² S. Ovchinnikov, *Physics-Uspechi* **40**, 993 (1997).
- ³³ R. O. Zaltsev, *JETP* **41**, 100 (1975).
- ³⁴ V. Y. Irkhin and Y. P. Irkhin, *JETP* **104**, 3868 (1993).
- ³⁵ V. Y. Irkhin and Y. P. Irkhin, *Phys. Stat. Sol. (b)* **183**, 9 (1994).
- ³⁶ V. A. Gavrichkov, Z. V. Pchelkina, I. A. Nekrasov, and S. G. Ovchinnikov, *International Journal of Modern Physics B* **30**, 1650180 (2016).
- ³⁷ V. A. Gavrichkov and S. G. Ovchinnikov, *Fiz.Tverd.Tela* **50**, 1037 (2008).
- ³⁸ S. G. Ovchinnikov, *JETP* **107**, 140146 (2008).
- ³⁹ A. Y. Kuznetsov, J. Almeida, L. Dubrovinsky, R. Ahuja, S. K. Kwon, I. Kantor, and N. Guignot, *Journal of Applied Physics* **99(5)**, 053909 (2006).
- ⁴⁰ J.-S. Zhou, J. A. Alonso, A. Muoz, M. T. Fernandez-Diaz, and J. B. Goodenough, *Phys. Rev. Lett.* **106**, 057201 (2011).
- ⁴¹ J.-S. Zhou and J. B. Goodenough, *Phys. Rev. Lett.* **89**, 087201 (2002).
- ⁴² A. G. Gavriiliuk, I. A. Trojan, S. G. Ovchinnikov, I. S. Lyubutin, and V. A. Sarkisyan, *JETP* **99**, 566573 (2004).
- ⁴³ I. S. Lyubutin and S. G. Ovchinnikov, *JMMM* **324**, 35383541 (2012).
- ⁴⁴ I. S. Lyubutin, V. V. Struzhkin, A. A. Mironovich, A. G. Gavriiliuk, P. G. Naumov, J. F. Lin, S. G. Ovchinnikov, S. Sinogeikin, P. Chow, Y. Xiao, and R. J. Hemley, *Proceedings of National Academy of Science of USA (PNAS)* **110(18)**, 7142 (2013).
- ⁴⁵ W. Jauch, M. Reehuis, H. J. Bleif, F. Kubanek, and P. Pattison, *Phys. Rev. B* **64**, 052102 (2001).
- ⁴⁶ T. Atou, M. Kawasaki, and S. Nakajima, *Jpn. J. Appl. Phys.* **43**, L1281L1283 (2004).
- ⁴⁷ Q. Guo, H.-K. Mao, J. Hu, J. Shu, and R. J. Hemley, *J. Phys.: Condens. Matter* **14**, 11369 11374 (2002).
- ⁴⁸ N. Rinaldi-Montes, P. Gorria, D. Martinez-Blanco, A. B. Fuertes, Puente-Orench, L. Olivi, and J. A. Blanco, *AIP Advances* **6**, 056104 (2016).
- ⁴⁹ K. I. Kugel and D. I. Khomskii, *Sov. Phys. Usp.* **25(4)**, 231 (1982).
- ⁵⁰ S. V. Streltsov and D. I. Khomskii, *Phys. Usp.* **60**, 1121 (2017).
- ⁵¹ K. Yamada, M. Matsuda, Y. Endoh, B. Keimer, R. J. Birgeneau, S. Onodera, J. Mizusaki, T. Matsura, and G. Shirane, *Phys. Rev. B* **39**, 2336 (1989).
- ⁵² R. D. Sanchez, M. T. Causa, A. Caneiro, A. Butera, M. Vallet-Regi, M. J. Sayagues, J. Gonzalez-Calbet, F. Garcia-Sanz, and J. Rivas, *Phys. Rev. B* **54**, 16574 (1996).
- ⁵³ M. Golalikhani, Q. Lei, R. U. Chandrasena, L. Kasaei, H. Park, J. Bai, P. Orgiani, G. E. S. J. Ciston, D. A. Arena, P. Shafer, E. Arenholz, B. A. Davidson, A. J. Millis, A. X. Gray, and X. X. Xi, *Nat. Comm.* **9**, 2206 (2018).
- ⁵⁴ O. N. Lis, S. E. Kichanov, D. P. Kozlenko, Z. Jirak, A. V. Belushkin, and B. N. Savenko, *JMMM* **487**, 165360 (2019).
- ⁵⁵ Y. Drees, Z. W. Li, A. Ricci, M. Rotter, W. Schmidt, D. Lamago, O. Sobolev, U. Rutt, O. Gutowski, M. Sprung, A. Piovano, J. P. Castellán, and A. C. Komarek, *Nat. Comm.* **5**, 5731 (2014).
- ⁵⁶ A. P. Kampf, *Physics Reports* **249**, 219351 (1994).
- ⁵⁷ G. I. Bersuker, N. N. Gorinchoy, V. Z. Polinger, and A. O. Solonenko, *Supercond.: Phys., Chem., Eng.* **5**, 1003 (1992).
- ⁵⁸ Q. Si and E. Abrahams, *PRL* **101**, 076401 (2008).
- ⁵⁹ T. Saitoh, D. S. Dessau, Y. Morimoto, T. Kimura, Y. Tokura, and N. Hamada, *Phys. Rev. B* **62**, 1039 (2000).
- ⁶⁰ M. Baldini, V. V. Struzhkin, A. F. Goncharov, P. Postorino, and W. L. Mao, *Phys. Rev. Lett.* **106**, 066402 (2011).
- ⁶¹ B. S. Shastry, *Phys. Rev. Lett.* **63**, 1288 (1989).
- ⁶² L. F. Feiner, J. H. Jefferson, and R. Raimondi, *Phys. Rev. B* **53**, 8751 (1996).
- ⁶³ V. A. Gavrichkov, S. G. Ovchinnikov, and L. E. Yakimov, *JETP* **102**, 972985 (2006).